

# Type I-(BC<sub>2</sub>N)<sub>12</sub> Alkali Metal Endohedral Nanocages: DFT Global Reactivity Indexes, Gas and Aqueous Phase

Nima Karachi<sup>1</sup>, Asadollah Boshra<sup>2</sup>

<sup>1</sup> Chemistry Department, Marvdasht Branch, Islamic Azad University, Marvdasht, Iran

<sup>2</sup> Chemistry Department, Boroujerd Branch, Islamic Azad University, Boroujerd, Iran

**Corresponding author:**

Nima Karachi

مجله علمی پژوهش در شیمی و مهندسی شیمی (سال اول)  
شماره ۱۱ / پاییز ۱۳۹۶ / ص ۴۳-۵۰

## Abstract

The study deals with DFT based chemical reactivity parameters of type I-(BC<sub>2</sub>N)<sub>12</sub> alkaline endohedral nanocages as a possible molecular engineering. The computations were performed both in gas and aqueous phases through IEFPCM formalism. The structure and electronic properties of endohedral Type I-(BC<sub>2</sub>N)<sub>12</sub> nanocages have been investigated as a function of alkali atom inside the nanocage using density functional theory. We have calculated and analyzed basic characteristic related to the reactivity behavior, such as HOMO-LUMO band gap, chemical hardness, chemical potential, as well as the global electrophilicity index,  $\omega(H,L)$  of the encapsulated Type I-(BC<sub>2</sub>N)<sub>12</sub> nanocages.

**Keywords:** Type I-(BC<sub>2</sub>N)<sub>12</sub> nanocage, Density functional theory, Chemical reactivity descriptors, IEFPCM

## Introduction

Heterostructure BCN compounds have been subjected to various experimental [1,2] and theoretical [3-5] studies due to their interesting properties. Several kinds of semiconductors can be expected from BCN materials as well. Arc-discharge methods were used to produce stable BC<sub>2</sub>N nanotubules structures [6]. Loeffler *et al* synthesized BCN coatings on Si (100) substrates by plasma-assisted chemical vapour deposition (PACVD) [7]. The B-C-N nanotubes grew by metal catalyzed laser ablation and characterized by scanning transmission electron microscopy and electron energy-loss spectroscopy [8]. Popov and coworkers deposited BCN films on monocrystalline silicon substrates by laser ablation [9]. Electric arc-discharge method were applied to synthesize concentric cylinders of BC<sub>2</sub>N nanotubes [10]. Watanabe *et al.* showed that a kind of synthesized BC<sub>2</sub>N structure has electronic properties intermediate between semi-metallic graphite and large-band-gap h-BN [11]. Amorphous BC<sub>2</sub>N semiconductors were prepared thorough mechanical milling with hexagonal boron nitride and graphite as starting materials [12]. A density functional theory study on cubic phases of BC<sub>2</sub>N synthesized experimentally showed that BC<sub>2</sub>N cubic phases are stable [13]. Oliaey *et al.* constructed novel (BC<sub>2</sub>N)<sub>12</sub> nanocages (Type-I, II, and III) [14] based upon theoretical studies of Kirin and D'yachkov BC<sub>2</sub>N nanotubes [15]. They showed that these novel BC<sub>2</sub>N nanocages are stable via density functional theory

In this study, DFT method were employed to study global chemical reactivity of endohedral derivatives of type I-(BC<sub>2</sub>N)<sub>12</sub> [14] nanocages. The encaged species were alkaline metals (Li, Na, and K) and also their cations. The calculations were carried out both in gas and aqueous phase.

Our aim is to use DFT calculated reactivity descriptors to predict and compare the reactivities of alkali encapsulated structures of type I-(BC<sub>2</sub>N)<sub>12</sub>, and their cations in gas and aqueous phases to develop novel nanostructures with new characteristics for diverse applications.

## Computational Details

At the first step we constructed type I-(BC<sub>2</sub>N)<sub>12</sub> nanocage, and its alkali metal atoms/ions (Li, Na and K) endohedral derivatives (Figure 1) as Oliaey *et al.* suggested [14]. Density functional theory (DFT) has been used to obtain equilibrium nanocage structures [16]. These structures were obtained using the B3LYP hybrid functional, which consists of a three-parameter hybrid functional (B3) as the exchange component [17] and a Lee-Yang-Parr (LYP) correlation function [18]. The B3LYP hybrid functional has produced reasonable results for BN cages [19] and their derivatives [20,21]. Also B3LYP with 3-21G basis set applied for BN substitution of fullerenes, C<sub>60-2x</sub>(BN)<sub>x</sub> to estimate HOMO-LUMO band gap and relative energies of the isomers [22,23].

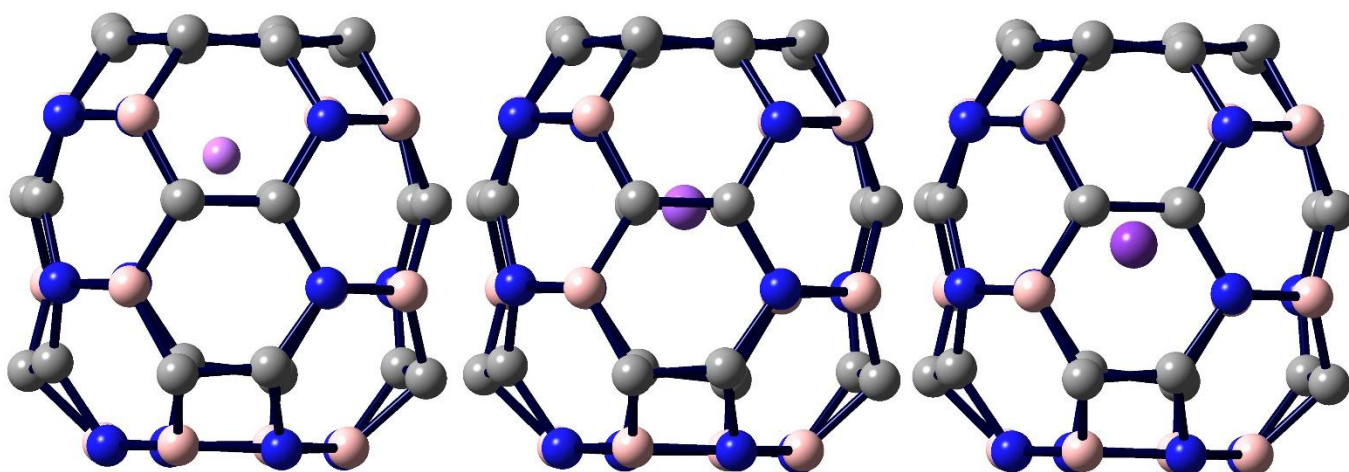


Fig 1. 3D representation of Type I-(BC<sub>2</sub>N)<sub>12</sub> alkali metal endohedral nanocages: [Li@I-(BC<sub>2</sub>N)<sub>12</sub>], [Na@I-(BC<sub>2</sub>N)<sub>12</sub>], and [K@I-(BC<sub>2</sub>N)<sub>12</sub>] (Left to right)

In this study, we use the B3LYP with 6-311+G(d) basis set [24,25] to optimize the endohedral nanocages geometries ([M@type I-(BC<sub>2</sub>N)<sub>12</sub>] and [M<sup>+</sup>@type I-(BC<sub>2</sub>N)<sub>12</sub>]). Band gaps were estimated by the energy difference between the highest occupied molecular orbital (HOMO) and the lowest unoccupied molecular orbital (LUMO). These orbitals are best termed Kohn-Sham (KS) orbitals when DFT methods are applied. Stowasser [26] and Hoffmann showed that the shapes and symmetries of the KS orbitals are fairly similar to those of the Hartree-Fock (HF) orbitals that are so familiar to chemists. The similarity between KS and HF orbitals has also been reported in several articles [27-29].

The definitions of various descriptors and their usefulness in the elucidation of structure-reactivity correlations have been elegantly highlighted in the recent reviews [30,31]. Parr et al. [32] have introduced the global electrophilicity index ( $\omega$ ) in terms of chemical potential and hardness as,

$$\omega(H, L) = \frac{\mu^2}{2\eta} \quad (1)$$

The global electrophilicity index measures the stabilization in energy when the system acquires an additional electronic charge  $\Delta N$  from the environment. This index is stated in terms of the electronic chemical potential  $\mu$  and the chemical hardness  $\eta$ . the global chemical reactivity was determined by applying the concept of electronegativity ( $\chi$ ) [33]. Another way to define electronegativity is through Mulliken's prescription [34]:

$$\mu = -\frac{(I + A)}{2} \quad (2)$$

Also chemical hardness ( $\eta$ ) in DFT (like electronic chemical potential,  $\mu$ ) is evaluated directly from the ionization energies ( $I$ ) and electron affinities energies ( $A$ )

$$\eta = I - A \quad (3)$$

The computations of the ionization potentials and the electron affinities resulted from Koopmans' theorem, respectively [35]:

$$I \approx -\varepsilon_{HOMO} \quad (4)$$

$$A \approx -\varepsilon_{LUMO} \quad (5)$$

To evaluate the effect of water solvent on the reactivity parameters of considered endohedral nanocages, we performed all the above mentioned calculations in aqueous phase (water solvent) through integral equation formalism variant of polarizable Continuum Model (PCM), as well [36,37]. We used the Gaussian 98 suite of programs to carry out all the calculations [38].

## Results and Discussions

The symmetry points groups of endohedrals type I-(BC<sub>2</sub>N)<sub>12</sub> nanocages, [M@(BC<sub>2</sub>N)<sub>12</sub>] (M=Li, Na, and K), and their cations [M@(BC<sub>2</sub>N)<sub>12</sub>]<sup>+</sup> are shown in Table 1 (Figure 1). The point groups can reveal the probable shifting of confined atom inside the nanocage moving from gas to aqueous phase. As Table shows, all endohedral nanocages, and their cations in gas phase have symmetry point groups of C<sub>4</sub>. Table 1 also shows that the symmetry point groups of cages moving from gas phase to aqueous phase have been converted from C<sub>4</sub> to C<sub>1</sub> in structures in which encaged atoms are Li and Na. While the structure of type I-(BC<sub>2</sub>N)<sub>12</sub> shell in mentioned endohedrals remains intact, it can be concluded that Li and Na atoms have been shifted inside the cage due to solvation of related endohedrals and their cations in aqueous phase. When we look at the symmetry points groups of [K@(BC<sub>2</sub>N)<sub>12</sub>] and its cation we realize that the symmetry of these structures retain the same (C<sub>4</sub>) in both gas and aqueous phases revealing very slight or no shifting of encaged K/K<sup>+</sup> in the inner space of (BC<sub>2</sub>N)<sub>12</sub> cage through phase changing.

**Table 1.** Point-group symmetry, Total electronic energy (in a.u.),  $\Delta E$  (aqueous phase energy relative to gas phase energy of endohedral nanocage) (kcal/mol), nanocage dipole moment (in Debye), and boundary orbitals gaps computed via B3LYP/6-311+G(d) model chemistry of equilibrium geometry of models<sup>a, b</sup>

| Nanocage   | Symm. | TEE         | $\Delta E$ (solv) | Dipole Moment | E <sub>g</sub> (eV) |
|--|-------|-------------|-------------------|---------------|---------------------|
| [Li@(BC <sub>2</sub> N) <sub>12</sub> ]              | C4    | -1877.73843 | -19.704           | 1.26          | 2.50                |
|  | C1    | -1877.76983 |                   | 2.57          | 2.50                |
| [Li@(BC <sub>2</sub> N) <sub>12</sub> ] <sup>+</sup> | C4    | -1877.51638 | -59.344           | 16.23         | 2.76                |
|  | C1    | -1877.61095 |                   | 15.46         | 2.93                |
| [Na@(BC <sub>2</sub> N) <sub>12</sub> ]              | C4    | -2032.51166 | -15.863           | 2.40          | 2.38                |
|  | C1    | -2032.53694 |                   | 4.60          | 2.44                |
| [Na@(BC <sub>2</sub> N) <sub>12</sub> ] <sup>+</sup> | C4    | -2032.29783 | -51.180           | 16.23         | 3.09                |
|  | C1    | -2032.37939 |                   | 15.46         | 3.06                |
| [K@(BC <sub>2</sub> N) <sub>12</sub> ]               | C4    | -2470.14539 | -6.357            | 3.10          | 2.30                |
|  | C4    | -2470.15552 |                   | 5.02          | 2.39                |
| [K@(BC <sub>2</sub> N) <sub>12</sub> ] <sup>+</sup>  | C4    | -2469.93577 | -38.397           | 16.76         | 3.10                |
|  | C4    | -2469.99696 |                   | 16.83         | 3.11                |

<sup>a</sup> For more details refer to Fig 1.

<sup>b</sup> Each cell with two numbers indicates the parameters in gas, and aqueous phase, respectively

Table 1 collects the total electronic energies of each endohedral type I-(BC<sub>2</sub>N)<sub>12</sub> calculated via DFT. The energies can be used as a criterion for energy of solvation of considered endohedral nanocages to calculate the relative energy of solvation. The relative energy of solvation between gas phase and aqueous phase is defined as  $\Delta E(\text{solv})=E(\text{aq})-E(\text{g})$ . The symbols aq and g are referring to aqueous and gas phase respectively.

All relative energies of solvations,  $\Delta E(\text{solv})$  of endohedral structures are shown in Table 1. At a glance we can see that all relative energies of solvation are negative signed meaning the solvation of mentioned endohedrals ([M@(BC<sub>2</sub>N)<sub>12</sub>] and [M@(BC<sub>2</sub>N)<sub>12</sub>]<sup>+</sup>) are energetically favorable. A closer look at  $\Delta E(\text{solv})$  of endohedrals reveals that in each case, the solvation of endohedral cation ([M@(BC<sub>2</sub>N)<sub>12</sub>]<sup>+</sup>) is more favorable than its neutral structure ([M@(BC<sub>2</sub>N)<sub>12</sub>]). The observation looks obvious because the aqueous phase which is made up water molecules is polar and, the charged species (cations/anions) are solvated much better than their neutral structures. [Li@(BC<sub>2</sub>N)<sub>12</sub>] shows the largest relative energy of solvation among neutral nanocages, and there is a decreasing order moving from Li to K endohedral (Table 1). Evaluating the relative energies of solvation for cations of endohedral structures shows the same order. [Li@(BC<sub>2</sub>N)<sub>12</sub>]<sup>+</sup> with the relative energy of solvation of  $\Delta E(\text{solv})=-59.345$  kcal/mol is the best structure solvating in aqueous phase. On the other side, [K@(BC<sub>2</sub>N)<sub>12</sub>]<sup>+</sup> with  $\Delta E(\text{solv})=-38.397$  kcal/mol shows the least tendency to solvate in aqueous phase among cations.

One of the key characteristics of the chemical structures is electric dipole moment. The calculated dipole moments of endohedral type I-(BC<sub>2</sub>N)<sub>12</sub> nanocages (Table 1) show that for neutral nanostructures, [M@(BC<sub>2</sub>N)<sub>12</sub>] there is an increase in dipole moment of the nanocage. It means the solvation of the species with zero charge intensifies the molecular dipole moment of the endohedral nanocages. The difference between aqueous phase dipole moment and gas phase is the largest for [Li@(BC<sub>2</sub>N)<sub>12</sub>]. When it comes to dipole moments of cations of nanocages it can be seen that the [M@(BC<sub>2</sub>N)<sub>12</sub>]<sup>+</sup> nanocages are extraordinary highly polar, and the dipole moments are considerably larger than that of neutral nanocages [Li@(BC<sub>2</sub>N)<sub>12</sub>] in the similar phases (Table 1). It is worth mentioning that the dipole moments of [Li@(BC<sub>2</sub>N)<sub>12</sub>]<sup>+</sup> and [Na@(BC<sub>2</sub>N)<sub>12</sub>]<sup>+</sup> cations show a decrease moving from gas phase to aqueous phase (in contrast with what we observe for neutral endohedral nanocages). In this case [K@(BC<sub>2</sub>N)<sub>12</sub>]<sup>+</sup> is the exception due to slight increase of its dipole moment in aqueous phase (Table 1). Such extraordinary highly charged nanocages make their relative energies of solvations more favourable than those of neutral ones. As we can see there is not a clear and obvious relation among dipole moments and  $\Delta E(\text{solv})$ . In this case it may be useful to consider more parameters affecting solvation of chemical structures like polarizabilities of the structures, as well.

The calculated energy gaps of the models are collected in Table 1. The results indicate all the endohedrals type I-(BC<sub>2</sub>N)<sub>12</sub> nanocages as wide band semiconductors. Table 1 also shows that the changes in the band gaps of all endohedral nanocages between gas and aqueous phase are insignificant. Evaluating calculated band gaps of endohedral nanocages, and their cations shows that the cations band gaps are slightly larger. Table 1 also presents [Na@(BC<sub>2</sub>N)<sub>12</sub>]<sup>+</sup> and [K@(BC<sub>2</sub>N)<sub>12</sub>]<sup>+</sup> as semiconductors with the widest band gaps (3.06-3.11 eV) among the studied structures.

In Table 2 (see Figure 1), one can find the computed global electrophilicity indexes of the endohedrals type I-(BC<sub>2</sub>N)<sub>12</sub> nanocages and their related cations. There is no experimental data available for the mentioned parameters so this research might be a help for predicting chemical reactivities of these nanotubes.

The electronic chemical potential ' $\mu$ ' is a measure of the stabilization in energy obtained when the system acquires an additional electronic charge from the environment. Table 2 shows that the calculated electronic chemical potentials are negative for all considered endohedral nanocages. This observation shows that the models are favorably stabilized toward acquiring an additional electron from the environment. As Table 2 presents all electronic chemical potentials of the neutral species, [M@(BC<sub>2</sub>N)<sub>12</sub>] differ slightly, and in each structure the electronic chemical potential in aqueous phase has a smaller value although the difference is not meaningful again. [Li@(BC<sub>2</sub>N)<sub>12</sub>] with  $\mu=-4.46$  eV has the most favorable electronic potential in gas phase, and [K@(BC<sub>2</sub>N)<sub>12</sub>] has the most favorable electronic potential in aqueous phase ( $\mu=-4.23$  eV). The calculated electronic chemical potentials of the cations in gas phase are considerably larger than that of neutral ones. The values in the aqueous phase follows the same explained trend as well. Considering the electronic chemical potentials of the endohedral cations in gas and aqueous phase (Table 2) reveals that there is a considerable decrease in  $\mu$  values due to solvation in aqueous phase. The most favorable endohedral cation in gas phase acquiring an additional electronic charge from the environment is [Li@(BC<sub>2</sub>N)<sub>12</sub>]<sup>+</sup> ( $\mu=-8.42$  eV), and [K@(BC<sub>2</sub>N)<sub>12</sub>]<sup>+</sup> with chemical potential of -5.46 eV in aqueous phase (Table 2).

**Table 2. Chemical parameters indicative of the reactive behavior of the nanotube models calculated with the B3LYP/6-311+G(d) model chemistry<sup>a, b</sup>**

| Nanocage   | $\mu$ (eV) | $\eta$ (eV) | $\omega(H,L)$ (eV) |
|--|------------|-------------|--------------------|
| [Li@(BC <sub>2</sub> N) <sub>12</sub> ]              | -4.46      | 2.50        | 3.98               |
| [Li@(BC <sub>2</sub> N) <sub>12</sub> ] <sup>+</sup> | -4.16      | 2.50        | 3.46               |
| [Li@(BC <sub>2</sub> N) <sub>12</sub> ] <sup>+</sup> | -8.42      | 2.75        | 12.86              |
| [Li@(BC <sub>2</sub> N) <sub>12</sub> ] <sup>+</sup> | -5.37      | 2.93        | 4.93               |
| [Na@(BC <sub>2</sub> N) <sub>12</sub> ]              | -4.32      | 2.38        | 3.93               |
| [Na@(BC <sub>2</sub> N) <sub>12</sub> ]              | -4.14      | 2.44        | 3.52               |
| [Na@(BC <sub>2</sub> N) <sub>12</sub> ] <sup>+</sup> | -8.35      | 3.09        | 11.28              |
| [Na@(BC <sub>2</sub> N) <sub>12</sub> ] <sup>+</sup> | -5.43      | 3.06        | 4.81               |
| [K@(BC <sub>2</sub> N) <sub>12</sub> ]               | -4.27      | 2.30        | 3.95               |
| [K@(BC <sub>2</sub> N) <sub>12</sub> ]               | -4.23      | 2.39        | 3.75               |
| [K@(BC <sub>2</sub> N) <sub>12</sub> ] <sup>+</sup>  | -8.26      | 3.10        | 11.00              |
| [K@(BC <sub>2</sub> N) <sub>12</sub> ] <sup>+</sup>  | -5.46      | 3.11        | 4.80               |

<sup>a</sup> For additional details refer to Fig 1.<sup>b</sup> Each cell with two numbers indicates the parameters in gas, and aqueous phase, respectively

Referring to electronic chemical hardness  $\eta$  column of Table 2 (Figure 1) it is clarified that the most resistant neutral endohedral structure against charge transfer in both gas and aqueous phase is [Li@(BC<sub>2</sub>N)<sub>12</sub>] due to its largest value of  $\eta$  (2.50 eV). The structures [Na@(BC<sub>2</sub>N)<sub>12</sub>] and [K@(BC<sub>2</sub>N)<sub>12</sub>] have a slightly larger chemical hardness in aqueous phase in comparison of those in gas phase. There is an increase in chemical hardness of cation structures moving from [Li@(BC<sub>2</sub>N)<sub>12</sub>]<sup>+</sup> to [K@(BC<sub>2</sub>N)<sub>12</sub>]<sup>+</sup> meaning the hardest cation structure among the studied endohedral nanocages is [K@(BC<sub>2</sub>N)<sub>12</sub>]<sup>+</sup> both in gas (3.10 eV) and aqueous phase (3.11 eV). The Table also shows in each endohedral structure, the cation presents the harder structure behavior due to its larger calculated chemical hardness in gas and aqueous phase.

It turns out from Table 2 (Figure 1) that in the neutral endohedral nanocages the reactivities in the gas phase are larger than that of aqueous phase although the differences are not significant. The most reactive structure among neutral endohedral nanocages is [Li@(BC<sub>2</sub>N)<sub>12</sub>] with  $\omega(H,L)$ = 3.98 eV in gas phase. The calculated chemical reactivities of endohedral cations as Table 2 shows are larger than that of neutral ones. A closer look at chemical reactivities of [M@(BC<sub>2</sub>N)<sub>12</sub>]<sup>+</sup> species reveals that chemical reactivity indexes in the gas phase are much larger than that of in the aqueous phase. [Li@(BC<sub>2</sub>N)<sub>12</sub>]<sup>+</sup> structure with a chemical reactivity of 12.86 eV in gas phase, and 4.93 eV in aqueous phase is the most reactive endohedral nanocage cation.

## Conclusions

We have studied the total electronic energies, dipole moments, energy bands, and global reactivity descriptors of endohedral type I-(BC<sub>2</sub>N)<sub>12</sub> nanocages; [M@(BC<sub>2</sub>N)<sub>12</sub>] (M=Li, Na, and K), and their cations [M@(BC<sub>2</sub>N)<sub>12</sub>]<sup>+</sup> via density functional level of theory (i.e. B3LYP) with 6-311+G(d) basis sets. The calculations have performed both in gas and aqueous phase through IEFPCM formalism. The results of relative energies of solvations, ΔE(solv) verified solvation of endohedral nanocages in aqueous phase favorable. [Li@(BC<sub>2</sub>N)<sub>12</sub>]<sup>+</sup> nanocage was the best structure for solvation in aqueous phase. The cations of [M@(BC<sub>2</sub>N)<sub>12</sub>] nanocages were highly polar structures making them good choices for solvation in polar phases. All considered endohedral nanocages indicated as wide band gap semiconductors. The calculated reactivity descriptors of the structures showed that solvation of nanocages in aqueous phase results in a decrease in the reactivities of endohedral nanocages. This decrease was more tangible when we considered the cations. Among neutral endohedral nanocages, [Li@(BC<sub>2</sub>N)<sub>12</sub>] and [K@(BC<sub>2</sub>N)<sub>12</sub>] were the most reactive structures in gas and aqueous phase, respectively. The most reactive cation endohedral structure in both gas and aqueous phase was [Li@(BC<sub>2</sub>N)<sub>12</sub>]<sup>+</sup>.

## Acknowledgements

This work was funded entirely by Islamic Azad University, Marvdasht branch.

**References**

- [1] Kawaguchi, M. *Advanced Materials* 1997, 9, 615-625.
- [2] Terrones, M.; Grobert, N.; Terrones, H. *Carbon* 2002, 40, 1665-1684.
- [3] Tateyama, Y.; Ogitsu, T.; Kusakabe, K.; Tsuneyuki, S.; Itoh, S. *Physical Review B* 1997, 55, R10161.
- [4] Gal'pern, E.; Stankevich, I.; Chistyakov, A.; Chernozatonskii, L. *Russian chemical bulletin* 1999, 48, 428-432.
- [5] Blase, X.; Charlier, J.-C.; De Vita, A.; Car, R. *Applied Physics A* 1999, 68, 293-300.
- [6] Weng-Sieh, Z.; Cherrey, K.; Chopra, N. G.; Blase, X.; Miyamoto, Y.; Rubio, A.; Cohen, M. L.; Louie, S. G.; Zettl, A.; Gronsky, R. *Physical Review B* 1995, 51, 11229-11232.
- [7] Loeffler, J.; Steinbach, F.; Bill, J.; Mayer, J.; Aldinger, F. *Metallkd* 1996 87, 170-174.
- [8] Zhang, Y.; Gu, H.; Suenaga, K.; Iijima, S. *Chemical physics letters* 1997, 279, 264-269.
- [9] Popov, C.; Ivanov, B.; Masseli, K.; Shanov, V. *Laser Physics* 1998, 8, 280-284.
- [10] Redlich, P.; Loeffler, J.; Ajayan, P.; Bill, J.; Aldinger, F.; Rühle, M. *Chemical physics letters* 1996, 260, 465-470.
- [11] Watanabe, M.; Sasaki, T.; Itoh, S.; Mizushima, K. *Thin Solid Films* 1996, 281, 334-336.
- [12] Yao, B.; Chen, W.; Liu, L.; Ding, B.; Su, W. *Journal of applied physics* 1998, 84, 1412-1415.
- [13] Kim, E.; Pang, T.; Utsumi, W.; Solozhenko, V. L.; Zhao, Y. *Physical Review B* ,۷۵ ,۲۰۰۷ ,۱۸۴۱۱۵
- [14] Olliaey, A. R.; Boshra, A.; Hamid, S. B. A. *Heteroatom Chemistry* 2015, 26, 150-160.
- [15] Kirin, D.; D'yachkov, P. *Doklady Physical Chemistry*, 2001, pp 227-233.
- [16] Becke, A. D. *J Chem Phys* 1993, 98, 5648-5652.
- [17] Lee, C.; Yang, W.; Parr, R. G. *Phys Rev B* 1988, 37, 785-789.
- [18] Hohenberg, P.; Kohn, W. *Phys Rev B* 1964, 136, 864-871.
- [19] Wu, H.-S.; Xu, X. H.; Zhang, F. Q.; Jiao, H. J. *J Phys Chem A* 2003 107 6609- 6612.
- [20] Cui, X.-Y.; Yang, B.-S.; Wu, H.-S. *Journal of Molecular Structure: THEOCHEM* 2010, 941, 144-149.
- [21] Wang, H.; Jia, J.-F.; Pei, X.-Q.; Wu, H.-S. *Chemical physics letters* 2006, 423, 118-122.
- [22] Pattanayak, J.; Kar, T.; Scheiner, S. *J Phys Chem A* 2001, 105, 8376-8384.
- [23] Pattanayak, J.; Kar, T.; Scheiner, S. *J Phys Chem A* 2002, 106, 2970-2978.
- [24] Hariharan, P. C.; Pople, J. A. *Theoretical Chemistry Accounts: Theory, Computation, and Modeling (Theoretica Chimica Acta)* 1973, 28, 213-222.
- [25] Clark, T.; Chandrasekhar, J.; Spitznagel, G. W.; Schleyer, P. V. R. *Journal of Computational Chemistry* 1983, 4, 294-301.
- [26] Stowasser, R.; Hoffmann, R. *Journal of the American Chemical Society* 1999, 121, 3414-3420.
- [27] Yang, W.; Mortier, W. J. *Journal of the American Chemical Society* 1986, 108, 5708-5711.
- [28] Hoffmann, R. *Journal of Molecular Structure: THEOCHEM* 1998, 424, 1-6.
- [29] [Kar, T.; Ángyán, J. G.; Sannigrahi, A. *The Journal of Physical Chemistry A* 2000, 104, 9953-9963.
- [30] Chermette, H. *Journal of Computational Chemistry* 1999, 20, 129-154.
- [31] Geerlings, P.; De Proft, F.; Langenaeker, W. *Chemical reviews* 2003, 103, 1793-1874.
- [32] Parr, R. G.; Szentpaly, L. v.; Liu, S. *Journal of the American Chemical Society* 1999, 121, 1922-1924.
- [33] Parr, R. G.; Donnelly, R. A.; Levy, M.; Palke, W. E. *The Journal of Chemical Physics* 1978, 68, 3801-3807.
- [34] Mulliken, R. S. *The Journal of Chemical Physics* 1934, 2, 782-793.
- [35] Koopmans, T. *Physica* 1933, 1, 104-113.
- [36] Miertuš, S.; Scrocco, E.; Tomasi, J. *Chemical Physics* 1981, 55, 117-129.
- [37] Cossi, M.; Barone, V.; Cammi, R.; Tomasi, J. *Chemical Physics Letters* 1996, 255, 327-335.
- [38] Frisch, M. J.; Trucks, G. W.; Schlegel, H. B.; Scuseria, G. E.; , R., M A; Cheeseman, J. R.; Zakrzewski, V. G.; Montgomery, J. A. J.; Stratmann, R. E.; Burant, J. C.; Dapprich, S.; Millam, J. M.; Daniels, A. D.; Kudin, K. N.; Strain, M. C.; Farkas, O.; Tomasi, J.; Barone, V.; Cossi, M.; Cammi, R.; Mennucci, B.; Pomelli, C.; Adamo, C.; Clifford, S.; Ochterski, J.; Petersson, G. A.; Ayala, P. Y.; Cui, Q.; Morokuma, K.; Malick, D. K.; Rabuck, A. D.; Raghavachari, K;

Foresman, J. B.; Cioslowski, J.; Ortiz, J. V.; Baboul, A. G.; Stefanov, B. B.; Liu, G.; Liashenko, A.; Piskorz, P.; Komaromi, I.; Gomperts, R.; Martin, R. L.; Fox, D. J.; Keith, T.; Al-Laham, M.; Peng, C. Y.; Nanayakkara, A.; Gonzalez, C.; Challacombe, M.; Gill, P. M. W.; Johnson, B.; Chen, W.; Wong, M. W.; Andres, J. L.; Gonzalez, C.; Head-Gordon, M.; Replogle, E. S.; Pople, J. A. Gaussian 98, revision A.7.; Gaussian, Inc.: Pittsburgh, PA, 1998.